Received: 16 February 2022 | Revised: 23 April 2022 | Accepted: 30 April 2022

DOI: 10.1002/aoc.6721

FULL PAPER

Applied Organometallic Chemistry WILEY

Pristine and alkali and alkaline earth metals encapsulated $B_{36}N_{36}$ nanoclusters as prospective delivery agents and detectors for 5-fluorouracil anticancer drug

Ehsan Shakerzadeh[1] | **Krzysztof K. Zborowski**[2] | **Ernesto Chigo Anota**[3] | **Minh Tho Nguyen**[4]

[1]Chemistry Department, Faculty of Science, Shahid Chamran University of Ahvaz, Ahvaz, Iran

[2]Department of General Chemistry, Faculty of Chemistry, Jagiellonian University, Kraków, Poland

[3]Benemérita Universidad Autónoma de Puebla, Facultad de Ingeniería Química, Ciudad Universitaria, Puebla, Mexico

[4]Institute for Computational Science and Technology (ICST), Ho Chi Minh City, Vietnam

Correspondence
Ehsan Shakerzadeh, Chemistry Department, Faculty of Science, Shahid Chamran University of Ahvaz, Ahvaz, Iran.
Email: e.shakerzadeh@scu.ac.ir

Funding information
Shahid Chamran University of Ahvaz, Grant/Award Number: SCU.SC1401.285

Quantum chemical investigation using density functional theory (DFT) approach is performed to assess the interactions of the anticancer 5-fluorouracil (FU) drug and $B_{36}N_{36}$ nanocluster. The alkali (AMs) and alkaline earth (AEMs) metals encapsulated $B_{36}N_{36}$ nanoclusters are also considered for FU adsorption. Results indicate the significant interaction of FU drug with pristine as well as encapsulated boron-nitride nanoclusters. Accordingly, the electronic structure of the nanoclusters is very sensitive to the FU adsorption. The resulting complexes have less energy gap than the bare ones, which can produce an appropriate signal for detection of the FU drug. Adsorption of six FU molecules on the top of each nanocluster indicates their high capacity for FU drug loading. The FU molecules also interact effectively with the AMs and AEMs encapsulated nanoclusters in the aqueous medium, which facilitates the drug delivery. The studied complexes have higher dipole moments in aqueous phase than in vacuum medium. The pristine and encapsulated $B_{36}N_{36}$ nanoclusters are suggested as prospective novel delivery agents and detectors for FU drug thanks of their suitable features.

KEYWORDS
5-fluorouracil, boron nitride nanocluster, DFT calculations, drug release, encapsulation

1 | INTRODUCTION

Recently, many biological applications of nanomaterials have been suggested[1–5] owing to their unique features and their dissimilarity as compared with their respective bulk counterparts. Among their various application, drug delivery systems using nanocarriers has provided the most promising approach.[6–13] For instance, Tayebee and coworkers studied various nanostructures as carriers for different anticancer drugs both experimentally and theoretically alike.[14–22] Boron nitride nanostructures are wide-band gap semiconductors with distinctive physico-chemical properties.[23,24] They are both chemically and thermally stable materials with high resistance to oxidation. Importantly, as boron nitride nanostructures are noncytotoxic and hydrophobic, they could be promising candidates for different biological applications and specifically in the nanomedicine field.

Spherical boron-nitride nanoclusters (BNNCs) were first synthesized in 1994,[25,26] and they have attracted many theoretical and experimental studies alike.[27–35] Oku et al.[26] reported that BN nanoclusters could efficiently be synthesized using an arc melting method. The existence of $B_{36}N_{36}$ and the singly doped $Y@B_{36}N_{36}$ derivatives was reported through high-resolution electron microscopy, mass spectrometry and characterized by

molecular mechanics and MO calculations.[36] The $B_{36}N_{36}$ nanocluster, with a fullerene-like structure, has been the subject of several theoretical studies.[37–45] Ganji et al.[46] studied the interaction between the $B_{36}N_{36}$ nanocluster and glycine amino acid using DFT approaches and suggested that it can be implemented as a novel material for drug delivery applications.

The 5-fluorouracil (FU) molecule has multiple applications[47] and is one of the most beneficial drugs to treat breast, head, neck, anal, stomach, colon and skin cancers.[48–50] Many studies have been dedicated to this multi-facet molecule obviously due to its efficient application as a chemotherapeutic agent.[51–55] Undoubtedly, nanomedicine is a revolutionary medical technology, particularly in the cancer therapy. In this treatment, the design of innovative drug delivery system is one of the most challenging tasks and thereby the survey of prospective drug delivery agents based on nanostructures constitutes a primordial subject. For instance, Namazi and coworkers reported the encapsulation of 5-fluorouracil into the porous of Zn-based metal–organic framework (MOF-5) as a bio-compatible drug delivery system for the colon cancer.[56] Gonzales et al. demonstrated that multi-walled carbon nanotubes complement the anti-tumoral effect of 5-fluorouracil, and it is a promising approach to boost the efficacy of traditional chemotherapies.[57] Furthermore, recent advances in the design of 5-fluorouracil delivery systems as a stepping stone in the safe treatment of colorectal cancer were reviewed by Entezar-Almahdi et al.[58] In view of the fact that experimental approaches inherently require high cost and longer time, computational studies can help experimentalists in the design of nanocarriers. The nature of the interactions between drugs and nanostructures emerges as an essential step. There are indeed several theoretical reports on the interactions of the FU molecule with different nano-based materials.[59–69]

In this context, we attempt in the present research to investigate the interactions of FU molecule with the $B_{36}N_{36}$ nanocluster. The evaluation of this process is important to understand and predict the role of nanoclusters as drug delivery systems. Furthermore, the effects of the alkali (Li, Na, K) and earth alkaline (Be, Mg, Ca) encapsulation inside the $B_{36}N_{36}$ nanocluster on the FU adsorption are subsequently studied.

2 | COMPUTATIONAL DETAILS

Quantum chemical calculations are carried out using the Accelrys' DMol^3 package.[70,71] All electronic structure calculations performed in this study are in the framework of density functional theory (DFT). Geometry optimization, adsorption energies, dipole moment, the Hirshfeld charge transfer, frontier molecular orbitals (HOMO–LUMO distribution), and *p*H-dependent release mechanism are considered to probe the interaction mechanism.

The generalized gradient approximation with the Becke and the Lee–Yang–Parr functional[72] (BLYP) in conjunction with a double numeric quality basis set (DNP) to ensure the accuracy of the calculations. This method was previously applied for studying of BN nanoclusters.[73] The van der Waals (vdW) interactions is also taken into account through the Grimme's dispersion-corrected (DFT + D) method.[74] The necessity for dispersion correction has been well documented for the adsorption energy calculations. The smearing parameter of 0.005 Ha and real-space orbital cutoff radius 4.5 Å were applied in all calculations. The geometry optimization are performed through the convergence criteria for the energy change, max force, and max displacement thresholds of 1×10^{-5} Hartree, 0.002 Hartree·Å^{-1}, and 0.005 Å, respectively. Harmonic vibrational frequency analyses were also carried out to verify the nature of local minima. Hirshfeld charge density method was applied for analyzing the charge-transfer process. The conductor-like screening model (COSMO) was applied for considering the solvent effect, as well as all computations are performed in the water phase ($\varepsilon = 78.54$).[75]

3 | RESULTS AND DISCUSSION

Figure 1 presents the optimized structures of the $B_{36}N_{36}$ nanocluster. Its HOMO and LUMO levels are located at −1.6 and −6.6 eV, respectively, resulting in a relatively large frontier orbital energy gap of 5.0 eV. Such a wide energy gap demonstrates its semiconductor feature, which well agrees with the experimental energy gap.[76] The $B_{36}N_{36}$ nanocluster consists of 6 four-membered rings and 32 six-membered rings, and thereby three kinds of B-N bonds can be distinguishable. The B666 bond (I in Figure 1) shares between two hexagons and both N and B atoms share three hexagons with the length of 1.49 Å. Another kind of bond is the B664 which is shared between two hexagons, but the B or N atom shares two hexagons, and one tetragonal ring with the length of 1.44 Å. The B64 one is shared between a tetragonal and a hexagon with a bond length of 1.47 Å, which well agrees with pervious report[43] (cf. Figure 1). All atomic sites are equivalent, as seen in the optimized structure of 5-fluorouracil shown in panel II of Figure 1. This drug contains two different types of oxygen atoms which are marked as O1and O2 in Figure 1. The bond lengths C1–O1 and C2–O1 amount to ∼1.23 Å.

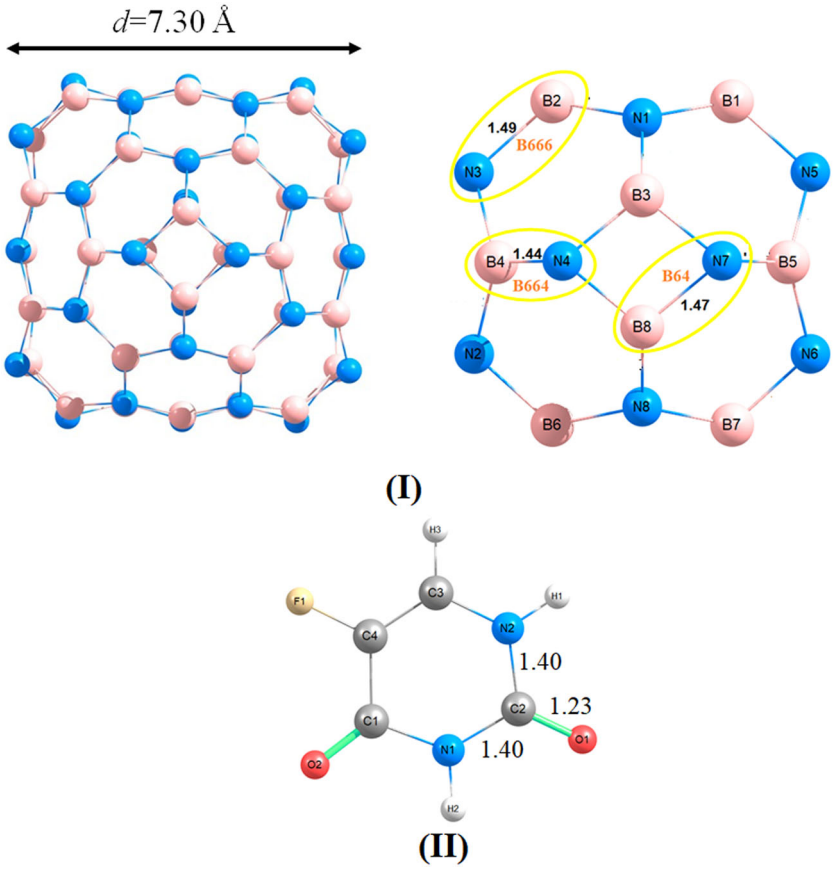

FIGURE 1 Optimized geometries of $B_{36}N_{36}$ and 5-fluoracil

Let us consider the adsorption behavior of FU on the surface of $B_{36}N_{36}$ nanocluster, which is expected to interact through positions with high electron density such as oxygen atoms. Different types of interaction for the resulting FU-$B_{36}N_{36}$ complex are examined. Accordingly, the FU molecule is located with different vertical or horizontal orientations on various positions of the $B_{36}N_{36}$ nanocluster, namely, atop of boron or nitrogen atom, center of tetragonal or hexagonal rings, and different B–N bonds with both orientations. After full geometry optimizations without any restrictions, the most stable complex is achieved whose the corresponding configuration involves a direct binding of a B atom of the nanocluster to the O1 center of FU (Figure 2). Because the boron atom has an empty valence orbital, it usually acts as a Lewis acid site for bonding with the lone pair electrons of the oxygen atoms. The interaction distance O1–B3 amounts to 1.63 Å. This interaction causes an elongation of B–N bonds. In fact, the B3–N4, B3–N7, and B3–N1 are elongated to 1.57, 1.53, and 1.50 Å, respectively. The B3–N4 bond seems to be much affected upon FU adsorption. Also, The C2–O1 bond of FU is stretched from 1.23 to 1.28 Å in FU-$B_{36}N_{36}$ complex, whereas the C2–N1 and C2–N2 bonds are slightly compressed from 1.40 to 1.37 Å.

The adsorption performance could be quantified by evaluation of the binding energy (E_{bin}) defined by Equation 1:

$$E_{bin} = E_{B_{36}N_{36}-FU} - \left(E^{iso}_{B_{36}N_{36}} + E^{iso}_{FU}\right), \quad (1)$$

where the $E_{B_{36}N_{36}-FU}$, $E^{iso}_{B_{36}N_{36}}$, and E^{iso}_{FU} terms correspond to the total electronic energy of the FU-$B_{36}N_{36}$ complex, the pristine $B_{36}N_{36}$ nanocluster, and the isolated FU molecule. It should be mentioned that it is not necessary to apply the basis set superposition error (BSSE) correction, because of the nearly complete basis set for the separated atoms, which is implemented in the program DMol^3.[77] As for a convention, a negative binding energy value stands for a thermodynamically favorable and exothermic adsorption of the FU drug onto the $B_{36}N_{36}$ nanocluster. The binding energy of the most stable FU-$B_{36}N_36$ complex is calculated to be −17.0 kcal/mol in vacuum. Table 1 provides the comparison of the binding energies of the FU interaction in gas phase with those of some other studied substrates. The binding energies of FU onto $B_{36}N_{36}$ nanocluster is larger than that of the B_{40} fullerene, monolayer BC_6N nanosheet, graphdiyne nanosheet, and $B_{24}N_{24}$ nanocluster. It is approximately similar to that of

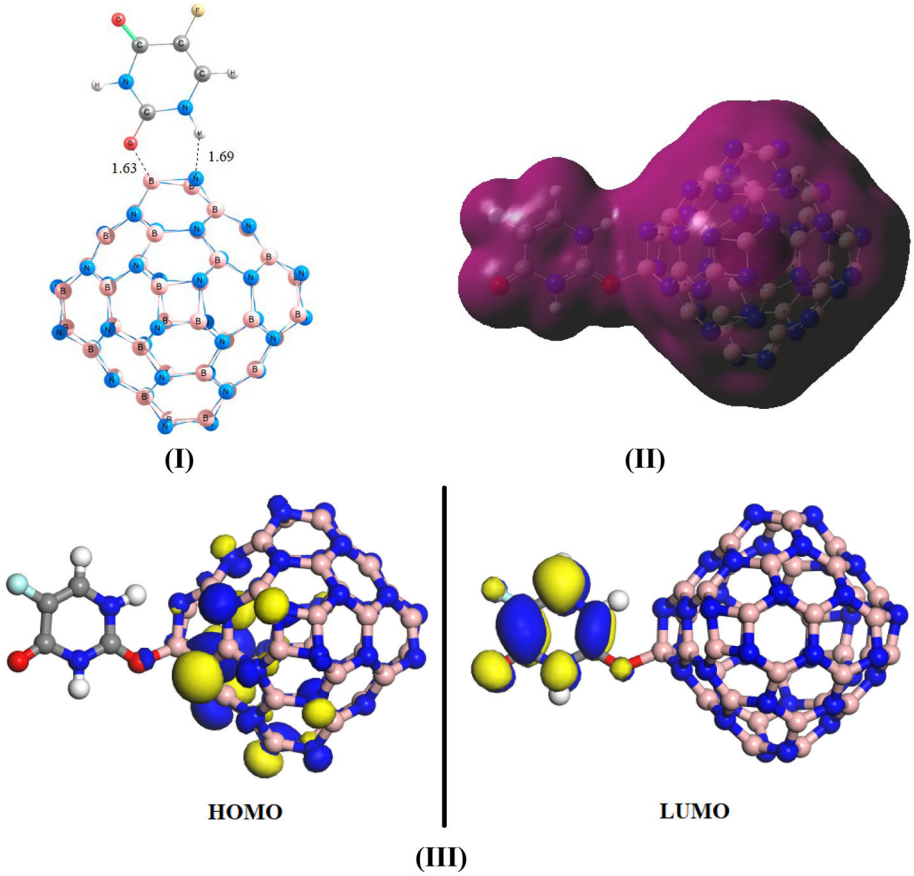

FIGURE 2 The obtained (I) most stable geometry, (II) total electron density map, and (III) the frontier molecular orbitals of FU-$B_{36}N_{36}$ complex

TABLE 1 Comparison of binding energy (kcal/mol) of FU-$B_{36}N_{36}$ complex in gas phase with reported literature values

Substrate	Method	Binding energy	Ref.
$B_{36}N_{36}$	PBE-D	−17.0	This work
B_{40} fullerene	PBE-D	−13.5	Shakerzadeh[69]
Monolayer BC_6N nanosheet	B3PW91	−13.83	Kaviani and Izadyar[63]
Graphdiyne nanosheet	B3LYP-D	−13.99	Yuan and Mohamadi[68]
$B_{24}N_{24}$ nanocluster	B3LYP-D	−11.90	Hazrati et al.[60]
2D-covalent triazine framework	M06-2X	−17.45	Fayyaz et al.[65]
Sumanene	B3LYP-D3	−17.14	Reichert et al.[64]
Cucurbit[6]urils	PBE-D	−19.37	Sabet and Ganji[61]
$Zn_{12}O_{12}$	B3LYP	−18.41	Zhihong et al.[14]
Boron carbide nanotube	M06-2X	−21.74	Cao et al.[66]
NC_3 carbon-like nanotube	B3LYP-D3	−20.83	Cao et al.[62]

the 2D-covalent triazine framework and sumanene, whereas it is smaller than the obtained values for cucurbit[6]urils $Zn_{12}O_{12}$, boron carbide nanotube, and NC_3 carbon-like nanotube.

The energy gap (E_g) value of the FU-$B_{36}N_{36}$ complex is decreased by 45% with respect to that the pristine $B_{36}N_{36}$ to a value of 2.8 eV. Thereby the adsorption of FU can be identified from such an electronic response, resulting in a decrease of electric conductivity. As illustrated in Figure 2, the LUMO level is located over the FU moiety in the FU-$B_{36}N_{36}$ complex, confirming the charge-flow tendency, going from FU to nanocluster. A more effective charge transfer within the FU-$B_{36}N_{36}$ complex corresponds to a better overlap between frontier orbitals of $B_{36}N_{36}$ and FU, resulting in a stronger interaction. Further insight can be obtained from the map of the

total electronic density. A significant overlap of electron clouds between the FU molecule and $B_{36}N_{36}$ nanocluster is observed from such total electron density calculation (cf. panel (II) in Figure 2). The net Hirshfeld charge of the FU molecule in FU- $B_{36}N_{36}$ complex is also computed to be ~0.28 a.u. Noticeably, the O1 atom of FU bears a net negative charge of −0.29 au in the isolated form, and it decreases to −0.13 au in FU-$B_{36}N_{36}$ complex. In this regard, the FU molecule acts as a Lewis acid whereas the nanocluster plays of course the role of a Lewis base.

Regarding the capacity of $B_{36}N_{36}$ for adsorption of FU, our computations demonstrate that it can carry up to six FU molecule simultaneously. The relaxed 6FU-$B_{36}N_{36}$ system is depicted in Figure S1 in the Supplementary materials. The binding energy per FU $(\overline{E}_{bin})$ in the 6FU-$B_{36}N_{36}$ complex is calculated to be −16.0 kcal/mol, according to the following equation:

$$\overline{E}_{bin} = \frac{1}{6}E_{6FU-B_{36}N_{36}} - \left(E^{iso}_{B_{36}N_{36}} + 6E^{iso}_{FU}\right). \quad (2)$$

The large adsorption energy per FU indicates that the $B_{36}N_{36}$ nanocluster would be an appropriate drug carrier with high capacity. However, this interaction needs to be considered in an aqueous medium for its compatibility as a drug delivery system in human body. When the effects of aqueous solution are included through the COSMO model, the binding energy per FU molecule in the 6FU-$B_{36}N_{36}$ complex becomes much more negative, namely, E_{bin} = − 31.4 kcal/mol. Moreover, the energy gap is distinctly decreased for this complex. The 6FU-$B_{36}N_{36}$ system has a value E_g = 2.2 eV in the gas phase and E_g = 2.7 eV in aqueous solution.

We now examine the effects of alkaline earth metal encapsulation inside the $B_{36}N_{36}$ cage on the FU adsorption behavior. Previous experimental reports demonstrated that a dark contrast is often observed near the center of the boron-nitride clusters, which indicates the existence of an atom inside.[78] Each metal is now put at the center of the $B_{36}N_{36}$ nanocluster and geometry optimizations are performed without any symmetry constraint. The spin multiplicity is a doublet for the AMs@$B_{36}N_{36}$ and a singlet for AEMs@$B_{36}N_{36}$. The AMs include the Li, Na, K elements, and the AEMs the Be, Mg, Ca. The encapsulation energy is computed as defined in Equation 3:

$$E_{Enc} = E_{M@B_{36}N_{36}} - \left(E^{iso}_{B_{36}N_{36}} + E^{iso}_{Metal}\right), \quad (3)$$

where the $E_{M@B_{36}N_{36}}$ and E^{iso}_{Metal} terms correspond to the total electronic energies of AMs or AEMs encapsulated $B_{36}N_{36}$ nanocluster (M@$B_{36}N_{36}$ with M = Li, Na, K, Be, Mg, and Ca) and free metal atom, respectively. The encapsulation energies are computed to be −21.2, −16.5, −17.1, −0.5, −2.9, and −3.5 kcal/mol for Li@$B_{36}N_{36}$, Na@$B_{36}N_{36}$, K@$B_{36}N_{36}$, Be@$B_{36}N_{36}$, Mg@$B_{36}N_{36}$, and

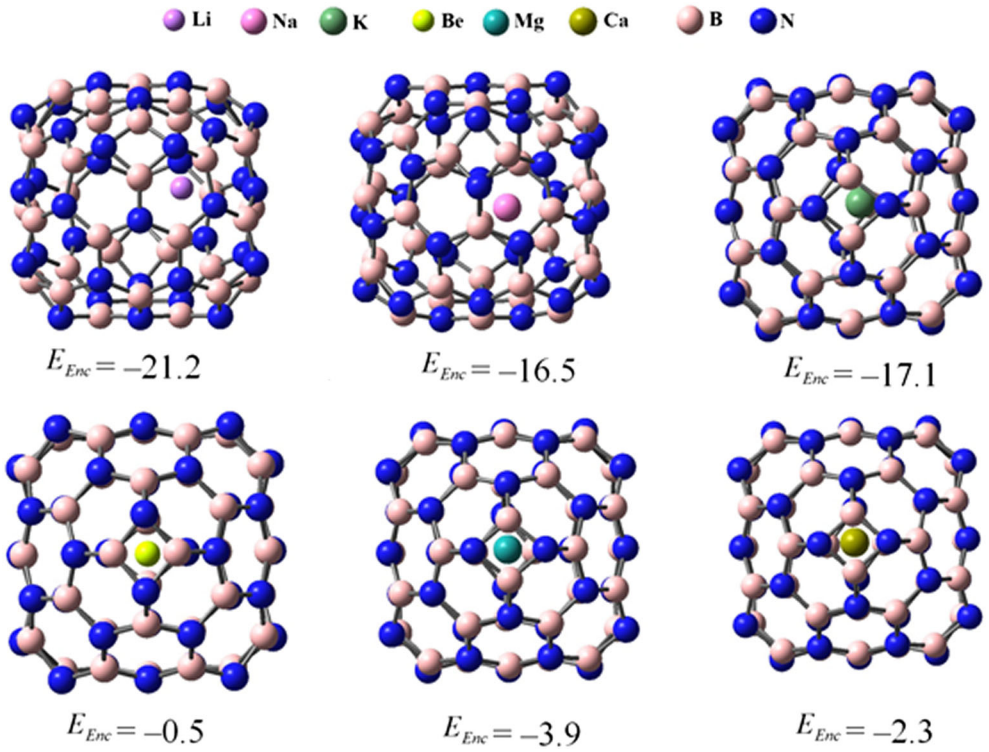

FIGURE 3 The AMs and AEMs encapsulated nanoclusters, and their encapsulation energies (E_{Enc}) given in kcal/mol

$Ca@B_{36}N_{36}$ nanoclusters, respectively, indicating a much higher thermodynamic stability of the alkali metal encapsulated nanoclusters in comparison with the alkaline earth metals counterparts. The relaxed structures of the encapsulated systems displayed in Figure 3 show that while the AEM is located at the center of the nanocluster, the AM is not. The Li element, being smaller in size, accurately fits within the cavity and exhibits the highest exothermic encapsulation energy among the considered systems.

Table 2 show that the HOMO and LUMO energies are fluctuated in all studied systems. The HOMO in all systems is destabilized and LUMO stabilized, which causes a narrowing in the HOMO-LUMPO gap (HLG) as compared the pristine $B_{36}N_{36}$ nanocluster. The destabilization of HOMO level in AM encapsulated system is very significant, resulting the greater HLGs with respect to AEMs encapsulated systems. The HLG values of $Li@B_{36}N_{36}$, $Na@B_{36}N_{36}$ and $K@B_{36}N_{36}$ systems reduce by 82, 85 and 96%, respectively; while the decreases for $Be@B_{36}N_{36}$, $Mg@B_{36}N_{36}$, and $Ca@B_{36}N_{36}$ correspond to 31%, 36%, and 74%.

For investigating the AMs and AEMs encapsulated $B_{36}N_{36}$ nanoclusters for FU adsorption, all possible positions of the encapsulated systems for the adsorption of the FU drugs are checked. The optimal number of the FU molecules adsorbed remains to be six as in the pristine nanocluster. The binding energy per FU molecule $(\overline{E}_{bin})$ is computed according to Equation 4:

$$\overline{E}_{bin} = \frac{1}{6}E_{6FU-M@B_{36}N_{36}} - (E_{M@B_{36}N_{36}} + 6E_{FU}). \quad (4)$$

The $E_{6FU-M@B_{36}N_{36}}$ term stands for the AM or AEM encapsulated $B_{36}N_{36}$ nanocluster, which is loaded by six FU molecules. The computed binding energies in both vacuum and aqueous medium, which are summarized in Table 3, are increased in gas phase as compared with that of pristine $B_{36}N_{36}$ ($\overline{E}_{bin} = -16.2$ kcal/mol for 6FU-$B_{36}N_{36}$ system) and the maximum binding energy correspond to 6FU-$K@B_{36}N_{36}$ system with $\overline{E}_{bin} = -24.9$ kcal/mol. Furthermore, the 6FU-$K@B_{36}N_{36}$ system has the highest $\overline{E}_{bin}$ in the aqueous medium (−36.5 kcal/mol) among the considered systems. It is worth mentioning that the $\overline{E}_{bin}$ values increase for in aqueous medium in comparison to the 6FU-$B_{36}N_{36}$. Importantly, the fact that the $\overline{E}_{bin}$ values in solution tend to increase with respect to the corresponding gas phase values points out the more effective interaction of FU with the metal encapsulated nanoclusters in the presence of water.

The atoms in molecules (AIM) theory[79] is a conventional computational approach for analyzing the nature of a chemical interaction using electron density distribution. The electron density at a bond critical point (BCP, ρ_{BCP}) and its Laplacian ($\nabla^2\rho_{BCP}$) are electron density parameters. The small value of electron density at a given BCP ($\rho_{BCP} \leq 0.20$) along with positive value of Laplacian of electron density at this point ($\nabla^2\rho_{BCP} > 0$) identify a van der Waals interaction.[80] For this purpose, the wave functions of the considered structures are constructed at BLYP/6-31G** using Gaussian 09 package[81] and AIM analyses are performed using the AIMALL software.[82] Accordingly, there are two BCPs (N ... H and B ... O) for the interaction of each FU drug with clusters. Therefore, six $BCPs_{(N...H)}$ and six $BCPs_{(B...O)}$ are observed for each studied system. The topological parameters

TABLE 2 The frontier molecular orbital energies (HOMO and LUMO), and HOMO-LUMO gap (HLG) with its relative variation (%ΔHLG)

	HOMO	LUMO	HLG	%ΔHLG
$B_{36}N_{36}$	−6.6	−1.6	5.0	
$Li@B_{36}N_{36}$	−2.7	−1.8	0.9	−82
$Na@B_{36}N_{36}$	−2.8	−2.1	0.7	−85
$K@B_{36}N_{36}$	−2.1	−1.9	0.2	−96
$Be@B_{36}N_{36}$	−6.1	−2.6	3.5	−31
$Mg@B_{36}N_{36}6$	−5.0	−1.7	3.2	−36
$Ca@B_{36}N_{36}$	−3.3	−2.0	1.3	−74

TABLE 3 The binding energy per FU molecule ($\overline{E}_{bin}$) and dipole moment (μ) for the studied systems in gas and water phases

	Gas phase		Water phase	
System	$\overline{E}_{bin}$ (kcal/mol)	μ (Debeye)	$\overline{E}_{bin}$ (kcal/mol)	μ (Debeye)
6FU-$B_{36}N_{36}$	−16.2	6.88	−31.4	11.11
6FU-$Li@B_{36}N_{36}$	−21.5	5.48	−33.7	9.93
6FU-$Na@B_{36}N_{36}$	−22.6	5.56	−34.8	9.78
6FU-$K@B_{36}N_{36}$	−24.9	6.07	−36.5	11.70
6FU-$Be@B_{36}N_{36}$	−16.6	6.82	−29.7	11.10
6FU-$Mg@B_{36}N_{36}$	−16.9	6.66	−29.7	11.18
6FU-$Ca@B_{36}N_{36}$	−22.0	5.06	−33.4	7.45

(ρ_{BCP} and $\nabla^2\rho_{BCP}$) are given in Table S1. Furthermore, the mean values of the ρ_{BCP} and $\nabla^2\rho_{BCP}$ for $BCPs_{(N...H)}$ and $BCPs_{(B...O)}$ are tabulated in Table 4. Accordingly, the existence of BCPs between the FU molecules and clusters confirms their chemical interaction. Accordingly, the considered BCPs have low electron density (ρ_{BCP}) together with positive $\nabla^2\rho_{BCP}$ values. Therefore, the van der Waals character of the interatomic contact is determined for the studied interactions.

The electronic dipole moment is an important issue for design of nanocarrier. The obtained electronic dipole moment (μ) values in both gas and water phases are tabulated in Table 2. While the dipole moment of the pristine $B_{36}N_{36}$ nanocluster is negligible (0.04 Debye), it increases significantly upon formation of the 6FU-$B_{36}N_{36}$ complex with the values of 6.9 and 11.1 Debye in gas and water phases, respectively. The adsorption of the FU molecules onto the metal encapsulated nanoclusters induces a remarkable increase of the resulting electronic dipole moment, in particular in aqueous solution. Such an enhancement of the dipole moment is very necessary for their solubility in a polar solvent such as water. An increase in the hydrophilicity after formation of the complex is valuable factor for the efficient drug delivery system.

TABLE 4 The calculated mean electron density properties of BCPs and bond lengths

Compound	Length (Å)	ρ_{BCP} (au)	$\nabla^2\rho_{BCP}$ (au)
$BCP_{(H...N)}$			
FU-$B_{36}N_{36}$	1.68	0.058	0.103
FU-Li@$B_{36}N_{36}$	1.76	0.048	0.102
FU-Na@$B_{36}N_{36}$	1.76	0.047	0.100
FU-K@$B_{36}N_{36}$	1.84	0.039	0.089
FU-Be@$B_{36}N_{36}$	1.68	0.058	0.103
FU-Mg@$B_{36}N_{36}$	1.68	0.058	0.103
FU-Ca@$B_{36}N_{36}$	1.81	0.043	0.095
$BCP_{(O...B)}$			
FU-$B_{36}N_{36}$	1.68	0.090	0.193
FU-Li@$B_{36}N_{36}$	1.61	0.104	0.291
FU-Na@$B_{36}N_{36}$	1.61	0.105	0.294
FU-K@$B_{36}N_{36}$	1.59	0.109	0.340
FU-Be@$B_{36}N_{36}$	1.68	0.090	0.192
FU-Mg@$B_{36}N_{36}$	1.67	0.091	0.205
FU-Ca@$B_{36}N_{36}$	1.59	0.110	0.341

For its part, a drug release from the carrier in the target cell is the most vital step in a drug delivery process. Owing to the excessive lactic production, a cancer cell has generally more acidic than normal cells (pH < 6).[83,84] Thus, it is necessary to evaluate the effect of the protons on the stability of the considered complexes. The most suitable positions for protonation of the FU molecule are obviously the O atoms, which are rich in electrons. Geometry optimizations of the protonated complexes are performed and the computed results indicate that the adsorption energies per protonated drug of the $B_{36}N_{36}$ and M@$B_{36}N_{36}$ decrease to about −10 kcal/mol in aqueous medium, which are less than that in the non-protonated complexes (being about −30 kcal/mol). Thus, a drug release from the introduced platforms could be possible in the vicinity of the cancer cells upon protonation is plausible.

Furthermore, the drug release can be occurred by exposing to light. The recovery time (τ) for the drug desorption from the cluster surface is computed based on the transition state theory[85] as follows:

$$\tau = \upsilon_0^{-1}\exp\left(\frac{-E_{bin}}{KT}\right),$$

TABLE 5 The time (in second) for the recovery of the FU drug from the cluster surfaces at 298 K

υ_0 (nm)	$B_{36}N_{36}$	Li@$B_{36}N_{36}$	Na@$B_{36}N_{36}$	K@$B_{36}N_{36}$	Be@$B_{36}N_{36}$	Mg@$B_{36}N_{36}$	Ca@$B_{36}N_{36}$
Gas phase							
10	2.7×10^{-5}	0.2	1.2	58.6	5.6×10^{-5}	7.8×10^{-5}	0.5
400	1.1×10^{-3}	8.5	47.3	2343.8	2.2×10^{-3}	3.1×10^{-3}	18.7
500	1.3×10^{-3}	10.6	59.2	2929.8	2.8×10^{-3}	3.9×10^{-3}	23.4
700	1.9×10^{-3}	14.7	82.6	4088.1	60270.1	5.4×10^{-3}	32.6
Aqueous medium							
10	3.9×10^{6}	1.7×10^{8}	1.2×10^{9}	2.0×10^{10}	2.0×10^{5}	2.0×10^{5}	1.1×10^{8}
400	1.5×10^{8}	6.7×10^{9}	4.8×10^{10}	8.0×10^{11}	7.5×10^{6}	7.5×10^{6}	4.2×10^{9}
500	1.9×10^{8}	8.4×10^{9}	6.0×10^{10}	1.0×10^{12}	9.9×10^{6}	9.9×10^{6}	5.6×10^{9}
700	2.0×10^{6}	1.2×10^{10}	8.4×10^{10}	1.4×10^{12}	1.3×10^{7}	1.3×10^{7}	7.9×10^{9}

where υ_0 is the attempt frequency. The temperature of the system and the Boltzmann constant denote by T and K terms, respectively. Accordingly, a larger binding energy causes a longer recovery time. Table 5 shows the times for drug release from the bare and encapsulated $B_{36}N_{36}$ surface at 298 K. In all cases, the recovery time in aqueous medium is very much longer than that in the gas phase. For instance, the recovery time of the FU drug from $B_{36}N_{36}$ is about 1.3×10^{-3} using the $\upsilon_0 = 500$ nm in gas phase, in comparison to 1.9×10^{8} seconds in aqueous phase.

4 | CONCLUDING REMARKS

The present research represents a primary but necessary contribution to the applications of $B_{36}N_{36}$ nanocluster for FU delivery and detection. Results reveal that the FU drug significantly interacts with both pristine and AMs- and AEMs-encapsulated boron-nitride nanoclusters in the range of approximately −16 to −24 kcal/mol in gas phase, and approximately −30 to −37 kcal/mol in aqueous continuum. The electronic structures of the nanoclusters are significantly affected upon interaction with FU. The frontier orbitals suggest the decrease of HLGs due to the FU drugs adsorption onto nanoclusters, indicating suitable electronic response for detection of FU drug. The binding of FU to the pristine and AMs and AEMs encapsulated $B_{36}N_{36}$ nanoclusters is expected to be reversible and triggered by the lower-shifted alteration of environment pH. The results altogether allow the pristine and encapsulated $B_{36}N_{36}$ nanoclusters to be considered as having a high potentiality for use as drug carriers and detectors, especially in cancer cells. We hope the results could open a new window in the nanomedicine domain.

ACKNOWLEDGMENT

This work was supported by Shahid Chamran University of Ahvaz, Ahvaz, Iran through Grant nr. SCU. SC1401.285.

AUTHOR CONTRIBUTIONS

Ehsan Shakerzadeh: Conceptualization; data curation; funding acquisition; investigation; methodology; software. **Krzysztof Zborowski:** Formal analysis; investigation; software. **Ernesto Chigo Anota:** Formal analysis; investigation; validation. **Minh Tho Nguyen:** Formal analysis; investigation; validation.

DATA AVAILABILITY STATEMENT

The data that supports the findings of this study are available in the supplementary material of this article.

ORCID

Ehsan Shakerzadeh https://orcid.org/0000-0003-1459-1481

Krzysztof K. Zborowski https://orcid.org/0000-0001-6042-2510

Ernesto Chigo Anota https://orcid.org/0000-0001-6037-7123

Minh Tho Nguyen https://orcid.org/0000-0002-3803-0569

REFERENCES

[1] R. M. Banciu, N. Numan, A. Vasilescu, *J. Mol. Struct.* **2022**, *1250*, 131639. https://doi.org/10.1016/j.molstruc.2021.131639

[2] M. Majeed, K. R. Hakeem, R. U. Rehman, *Chemosphere* **2022**, *288*, 132527. https://doi.org/10.1016/j.chemosphere.2021.132527

[3] O. Bashir, S. A. Bhat, A. Basharat, M. Qamar, S. A. Qamar, M. Bilal, H. M. N. Iqbal, *Chemosphere* **2022**, *292*, 133320. https://doi.org/10.1016/j.chemosphere.2021.133320

[4] H. Li, X. Wang, S. Wei, C. Zhao, X. Song, K. Xu, J. Li, B. Pang, J. Wang, *Anal. Chim. Acta* **2022**, *1190*, 338930. https://doi.org/10.1016/j.aca.2021.338930

[5] X. Bi, Q. Bai, L. Wang, F. Du, M. Liu, W. W. Yu, S. Li, J. Li, Z. Zhu, N. Sui, J. Zhang, *Nano Res.* **2022**, *15*, 1446. https://doi.org/10.1007/s12274-021-3685-4

[6] Z. Edis, J. Wang, M. K. Waqas, M. Ijaz, M. Ijaz, *Int. J. Nanomedicine* **2021**, *16*, 1313. https://doi.org/10.2147/IJN.S289443

[7] M. Kenchegowda, M. Rahamathulla, U. Hani, M. Y. Begum, S. Guruswamy, R. A. M. Osmani, M. P. Gowrav, S. Alshehri, M. M. Ghoneim, A. Alshlowi, D. V. Gowda, *Molecules* **2021**, *27*, 146. https://doi.org/10.3390/molecules27010146

[8] B. S. Alotaibi, M. Buabeid, N. A. Ibrahim, Z. J. Kharaba, M. Ijaz, S. Noreen, G. Murtaza, *Int. J. Nanomedicine* **2021**, *16*, 7517. https://doi.org/10.2147/IJN.S333657

[9] H.-R. Lan, Z.-Q. Wu, L.-H. Zhang, K.-T. Jin, S.-B. Wang, *Curr. Top. Med. Chem.* **2020**, *20*, 2442. https://doi.org/10.2174/1568026620666200722110808

[10] L. Kaur, H. S. Sohal, M. Kaur, D. S. Malhi, S. Garg, *Anticancer Agents Med Chem.* **2020**, *20*, 2012. https://doi.org/10.2174/1871520620666200804103714

[11] W. Wu, L. Luo, Y. Wang, Q. Wu, H.-B. Dai, J.-S. Li, C. Durkan, N. Wang, G.-X. Wang, *Theranostics.* **2018**, *8*, 3038. https://doi.org/10.7150/thno.23459

[12] R. Rahimi, M. Solimannejad, Z. Ehsanfar, *J. Mol. Model.* **2021**, *27*, 347. https://doi.org/10.1007/s00894-021-04930-x

[13] R. Rahimi, M. Solimannejad, M. Farghadani, *New J. Chem.* **2021**, *45*, 17976. https://doi.org/10.1039/d1nj03084a

[14] Y. Zhihong, Y. Ye, A. Pejhan, A. H. Nasr, N. Nourbakhsh, R. Tayebee, *Appl. Organomet. Chem.* **2020**, *34*, 1. https://doi.org/10.1002/aoc.5534

[15] M. Fu, R. Tayebee, S. Saberi, N. Nourbakhsh, E. Esmaeili, B. Maleki, H. R. Vatanpour, *Curr. Mol. Med.* **2021**, *21*, 698. https://doi.org/10.2174/1566524021666210111104428

[16] A. Sadat Hosseini Nasr, H. Akbarzadeh, R. Tayebee, *J. Mol. Liq.* **2018**, *254*, 64. https://doi.org/10.1016/j.molliq.2018.01.081

[17] R. Tayebee, A. H. Nasr, *J. Mol. Liq.* **2020**, *319*, 114357. https://doi.org/10.1016/j.molliq.2020.114357

[18] R. Guo, Q. Liu, W. Wang, R. Tayebee, F. Mollania, *J. Mol. Liq.* **2021**, *325*, 114798. https://doi.org/10.1016/j.molliq.2020.114798
[19] X. Dou, M. Keywanlu, R. Tayebee, B. Mahdavi, *J. Mol. Liq.* **2021**, *329*, 115557. https://doi.org/10.1016/j.molliq.2021.115557
[20] R. Tayebee, N. Zamand, A. Hosseini-Nasr, M. Kargar Razi, *J. Mol. Struct.* **2014**, *1065–1066*, 135. https://doi.org/10.1016/j.molstruc.2014.02.063
[21] R. Tayebee, A. Hosseini-nasr, N. Zamand, B. Maleki, *Polyhedron* **2015**, *102*, 503. 10.1016/j.poly.2015.10.022
[22] X. Xie, L. Zhang, W. Zhang, R. Tayebee, A. Hoseininasr, H. H. Vatanpour, Z. Behjati, S. Li, M. Nasrabadi, L. Liu, *J. Mol. Liq.* **2020**, *309*, 113024. 10.1016/j.molliq.2020.113024
[23] X. Li, D. Golberg, Chapter 5—Boron nitride nanotubes as drug carriers, in *Boron Nitride Nanotubes in Nanomedicine*, (Eds: G. Ciofani, V. Mattoli), William Andrew Publishing, Boston **2016** 79 10.1016/B978-0-323-38945-7.00005-5.
[24] A. Merlo, V. R. S. S. Mokkapati, S. Pandit, I. Mijakovic, *Biomater. Sci.* **2018**, *6*, 2298. https://doi.org/10.1039/c8bm00516h
[25] T. Oku, A. Nishiwaki, I. Narita, M. Gonda, *Chem. Phys. Lett.* **2003**, *380*, 620. https://doi.org/10.1016/j.cplett.2003.08.096
[26] T. Oku, A. Nishiwaki, I. Narita, *Sci. Technol. Adv. Mater.* **2004**, *5*, 635. https://doi.org/10.1016/j.stam.2004.03.017
[27] Z. Liao, G. Song, Z. Yang, H. Ren, *Mol. Phys.* **2021**, *119*, e1921296. https://doi.org/10.1080/00268976.2021.1921296
[28] H. Zhu, C. Zhao, Q. Cai, X. Fu, F. R. Sheykhahmad, *Inorg. Chem. Commun.* **2020**, *114*, 107808. https://doi.org/10.1016/j.inoche.2020.107808
[29] A. Bahrami, M. B. Qarai, N. L. Hadipour, *Theor. Chem.* **2017**, *1108*, 63. https://doi.org/10.1016/j.comptc.2017.03.018
[30] Y. Wang, L. Kang, *Catalysts* **2020**, *10*, 115. https://doi.org/10.3390/catal10010115
[31] O. V. de Oliveira, J. D. dos Santos, J. C. F. Silva, L. T. Costa, M. F. F. Junior, E. de Faria Franca, *Orbit* **2017**, *9*, 175. https://doi.org/10.17807/orbital.v9i3.991
[32] M. Rakib Hossain, M. Mehade Hasan, S. Ud Daula Shamim, T. Ferdous, M. Abul Hossain, F. Ahmed, *Comput. Theor. Chem.* **2021**, *1197*, 113156. https://doi.org/10.1016/j.comptc.2021.113156
[33] L. Mahdavian, *Polycyclic Aromat. Compd.* **2018**, *38*, 445. https://doi.org/10.1080/10406638.2016.1238399
[34] J. C. Escobar, M. S. Villanueva, A. B. Hernández, D. Cortés-Arriagada, E. C. Anota, *J. Mol. Graph. Model.* **2019**, *86*, 27. https://doi.org/10.1016/j.jmgm.2018.10.003
[35] E. Shakerzadeh, N. Barazesh, S. Z. Talebi, *Superlattices Microstruct.* **2014**, *76*, 264. https://doi.org/10.1016/j.spmi.2014.09.037
[36] T. Oku, I. Narita, A. Nishiwaki, *J. Phys. Chem. Solid* **2004**, *65*, 369. https://doi.org/10.1016/j.jpcs.2003.09.010
[37] X. Li, M. Ahmed, A. Surendar, R. Razavi, M. Najafi, *Mater. Chem. Phys.* **2019**, *223*, 694. https://doi.org/10.1016/j.matchemphys.2018.11.065
[38] H.-S. Wu, X.-H. Xu, D. L. Strout, H. Jiao, *J. Mol. Model.* **2005**, *12*, 1. https://doi.org/10.1007/s00894-005-0275-4
[39] A. Nishiwaki, T. Oku, K. Suganuma, *Phys. B* **2004**, *349*, 254. https://doi.org/10.1016/j.physb.2004.03.308
[40] I. Narita, T. Oku, *Diamond Relat. Mater.* **2002**, *11*, 945. https://doi.org/10.1016/S0925-9635(01)00536-2
[41] H. Xie, X. Wang, M. Wang, H. Pan, M. Najafi, *Monatshefte Fur Chemie.* **2019**, *150*, 1779. https://doi.org/10.1007/s00706-019-02492-6
[42] A. R. Oliaey, A. Boshra, *Phys. E Low-Dimensional Syst. Nanostructures.* **2013**, *52*, 136. https://doi.org/10.1016/j.physe.2013.03.011
[43] S. S. Alexandre, M. S. C. Mazzoni, H. Chacham, *Appl. Phys. Lett.* **1999**, *75*, 61. https://doi.org/10.1063/1.124277
[44] A. Surendar, A. Bozorgian, A. Maseleno, L. K. Ilyashenko, M. Najafi, *Inorg. Chem. Commun.* **2018**, *96*, 206. https://doi.org/10.1016/j.inoche.2018.08.025
[45] D. Farmanzadeh, H. Rezainejad, *Wuli Huaxue Xuebao/Acta Phys. - Chim. Sin.* **2016**, *32*, 1191. https://doi.org/10.3866/PKU.WHXB201603021
[46] M. D. Ganji, H. Yazdani, A. Mirnejad, *Phys. E Low-Dimensional Syst. Nanostructures.* **2010**, *42*, 2184. https://doi.org/10.1016/j.physe.2010.04.018
[47] J. L. Grem, *Invest. New Drugs* **2000**, *18*, 299. https://doi.org/10.1023/a:1006416410198
[48] F. Petrelli, M. Cabiddu, S. Barni, *Med. Oncol.* **2012**, *29*, 1020. https://doi.org/10.1007/s12032-011-9958-0
[49] S. Vodenkova, T. Buchler, K. Cervena, V. Veskrnova, P. Vodicka, V. Vymetalkova, *Pharmacol. Ther.* **2020**, *206*, 107447. https://doi.org/10.1016/j.pharmthera.2019.107447
[50] T. Searle, F. Al-Niaimi, F. R. Ali, *Dermatologic Surg.* **2021**, *47*, e66. https://doi.org/10.1097/DSS.0000000000002879
[51] M. F. Caminiti, M. El-Rabbany, J. Jeon, G. Bradley, *J. Oral Maxillofac. Surg.* **2021**, *79*, 814. https://doi.org/10.1016/j.joms.2020.07.215
[52] L. Maxfield, M. Shah, C. Schwartz, L. S. Tanner, J. Appel, *J. Am. Acad. Dermatol.* **2021**, *84*, 1696. https://doi.org/10.1016/j.jaad.2020.12.049
[53] J. Z. Almeida, L. F. Lima, L. A. Vieira, C. Maside, A. C. A. Ferreira, V. R. Araújo, A. B. G. Duarte, R. S. Raposo, S. N. Báo, C. C. Campello, L. F. S. Oliveira, T. P. da Costa, J. G. Abreu, J. R. Figueiredo, R. B. Oriá, *Cancer Chemother. Pharmacol.* **2021**, *87*, 567. https://doi.org/10.1007/s00280-020-04217-7
[54] H. Li, J. Lv, J. Guo, S. Wang, S. Liu, Y. Ma, Z. Liang, Y. Wang, W. Qi, W. Qiu, *Biochem. Biophys. Res. Commun.* **2021**, *540*, 108. https://doi.org/10.1016/j.bbrc.2021.01.006
[55] E. Shakerzadeh, *J. Mol. Liq.* **2017**, *240*, 682. https://doi.org/10.1016/j.molliq.2017.05.128
[56] S. Javanbakht, A. Hemmati, H. Namazi, A. Heydari, *Int. J. Biol. Macromol.* **2020**, *155*, 876. https://doi.org/10.1016/j.ijbiomac.2019.12.007
[57] E. González-Lavado, L. Valdivia, A. García-Castaño, F. González, C. Pesquera, R. Valiente, M. L. Fanarraga, *Oncotarget* **2019**, *10*, 2022. 10.18632/oncotarget.26770
[58] E. Entezar-Almahdi, S. Mohammadi-Samani, L. Tayebi, F. Farjadian, *Int. J. Nanomedicine* **2020**, *15*, 5445. https://doi.org/10.2147/IJN.S257700
[59] T. P. Alexandrovich, A. Khan, *Diamond Relat. Mater.* **2022**, *124*, 108900. https://doi.org/10.1016/j.diamond.2022.108900
[60] M. K. Hazrati, Z. Javanshir, Z. Bagheri, *J. Mol. Graph. Model.* **2017**, *77*, 17. https://doi.org/10.1016/j.jmgm.2017.08.003
[61] M. Sabet, M. D. Ganji, *J. Mol. Model.* **2013**, *19*, 4013. https://doi.org/10.1007/s00894-013-1936-3

[62] Y. Cao, H. A. Dhahad, H. M. Hussen, A. E. Anqi, N. Farouk, A. Issakhov, N.-Y. Xu, M. Derakhshandeh, *J. Mol. Liq.* **2021**, *340*, 117221. https://doi.org/10.1016/j.molliq.2021.117221
[63] S. Kaviani, M. Izadyar, *Mater. Chem. Phys.* **2022**, *276*, 125375. https://doi.org/10.1016/j.matchemphys.2021.125375
[64] T. Reichert, M. Vučićević, P. Hillman, M. Bleicher, S. J. Armaković, S. Armaković, *J. Mol. Liq.* **2021**, *342*, 117526. https://doi.org/10.1016/j.molliq.2021.117526
[65] F. Fayyaz, M. Yar, A. Gulzar, K. Ayub, *J. Mol. Liq.* **2022**, *356*, 118941. https://doi.org/10.1016/j.molliq.2022.118941
[66] Y. Cao, S. Alamri, A. A. Rajhi, A. E. Anqi, M. Derakhshandeh, *Mater. Chem. Phys.* **2022**, *275*, 125260. 10.1016/j.matchemphys.2021.125260
[67] Y. Yang, Z. Guangrong, W. Xiaojing, L. Wu, *Struct. Chem.* **2021**, *32*, 1. https://doi.org/10.1007/s11224-021-01779-x
[68] J. Yuan, A. Mohamadi, *J. Mol. Model.* **2021**, *27*, 1. https://doi.org/10.1007/s00894-020-04629-5
[69] E. Shakerzadeh, *J. Mol. Liq.* **2021**, *343*, 116970. https://doi.org/10.1016/j.molliq.2021.116970
[70] B. Delley, *J. Chem. Phys.* **1990**, *92*, 508. https://doi.org/10.1063/1.458452
[71] B. Delley, *J. Chem. Phys.* **2000**, *113*, 7756. https://doi.org/10.1063/1.1316015
[72] C. Lee, W. Yang, R. G. Parr, *Phys. Rev. B: Condens. Matter* **1988**, *37*, 785. https://doi.org/10.1103/physrevb.37.785
[73] X. Chen, J. Chang, H. Yan, D. Xia, *J. Phys. Chem. C* **2016**, *120*, 28912. https://doi.org/10.1021/acs.jpcc.6b08560
[74] S. Grimme, S. Ehrlich, L. Goerigk, *J. Comput. Chem.* **2011**, *32*, 1456. https://doi.org/10.1002/jcc.21759
[75] J. Andzelm, C. Kölmel, A. Klamt, *J. Chem. Phys.* **1995**, *103*, 9312. https://doi.org/10.1063/1.469990
[76] D. Golberg, Y. Bando, Y. Huang, T. Terao, M. Mitome, C. Tang, C. Zhi, *ACS Nano* **2010**, *4*, 2979. https://doi.org/10.1021/nn1006495
[77] Y. Inada, H. Orita, *J. Comput. Chem.* **2008**, *29*, 225. 10.1002/jcc.20782
[78] T. Oku, K. Suganuma, *Diamond Relat. Mater.* **2001**, *10*, 1205. https://doi.org/10.1016/S0925-9635(00)00392-7
[79] R. F. W. Bader, T. T. Nguyen-Dang, Quantum theory of atoms in molecules—Dalton revisited, in *Advances in Quantum Chemistry*, (Ed: P. O. Lowdin), Academic Press **1981** 63 10.1016/S0065-3276(08)60326-3.
[80] P. S. V. Kumar, V. Raghavendra, V. Subramanian, *J. Chem. Sci.* **2016**, *128*, 1527. https://doi.org/10.1007/s12039-016-1172-3
[81] M. J. Frisch, G. W. Trucks, H. B. Schlegel, G. E. Scuseria, M. A. Robb, J. R. Cheeseman, G. Scalmani, V. Barone, B. Mennucci, G. A. Petersson, H. Nakatsuji, M. Caricato, X. Li, H. P. Hratchian, A. F. Izmaylov, J. Bloino, G. Zheng, J. L. Sonnenberg, M. Hada, M. Ehara, K. Toyota, R. Fukuda, J. Hasegawa, M. Ishida, T. Nakajima, Y. Honda, O. Kitao, H. Nakai, T. Vreven, J. A. Montgomery, J. E. Peralta, F. Ogliaro, M. Bearpark, J. J. Heyd, E. Brothers, K. N. Kudin, V. N. Staroverov, R. Kobayashi, J. Normand, K. Raghavachari, A. Rendell, J. C. Burant, S. S. Iyengar, J. Tomasi, M. Cossi, N. Rega, J. M. Millam, M. Klene, J. E. Knox, J. B. Cross, V. Bakken, C. Adamo, J. Jaramillo, R. Gomperts, R. E. Stratmann, O. Yazyev, A. J. Austin, R. Cammi, C. Pomelli, J. W. Ochterski, R. L. Martin, K. Morokuma, V. G. Zakrzewski, G. A. Voth, P. Salvador, J. J. Dannenberg, S. Dapprich, A. D. Daniels, Ö. Farkas, J. B. Foresman, J. V. Ortiz, J. Cioslowski, D. J. Fox, *Gaussian 09 Revision A.2*, Gaussian, Inc. **2009**.
[82] R. Raccichini, A. Varzi, S. Passerini, B. Scrosati, *Nat. Mater.* **2015**, *14*, 271. https://doi.org/10.1038/nmat4170
[83] R. Rahimi, M. Solimannejad, Z. Ehsanfar, *Mol. Phys.* **2021**, *120*, e2014587. https://doi.org/10.1080/00268976.2021.2014587
[84] N. T. Si, N. T. A. Nhung, T. Q. Bui, M. T. Nguyen, P. V. Nhat, *RSC Adv.* **2021**, *11*, 16619. https://doi.org/10.1039/d1ra02172a
[85] S. Peng, K. Cho, P. Qi, H. Dai, *Chem. Phys. Lett.* **2004**, *387*, 271. https://doi.org/10.1016/j.cplett.2004.02.026

SUPPORTING INFORMATION

Additional supporting information may be found in the online version of the article at the publisher's website.

How to cite this article: E. Shakerzadeh, K. K. Zborowski, E. C. Anota, M. T. Nguyen, *Appl Organomet Chem* **2022**, e6721. https://doi.org/10.1002/aoc.6721